AD-A075 945 NAVAL OCEAN SYSTEMS CENTER SAN DIEGO CA F/G 17/1
UNDERWATER SOUND MATHEMATICAL MODEL. THEORETICAL DISCUSSION.(U)
AUG 79 R BELL
UNCLASSIFIED NOSC/TD-272 NL

1 OF 1
AD
A075945

END
DATE
FILMED
11-79
DDC

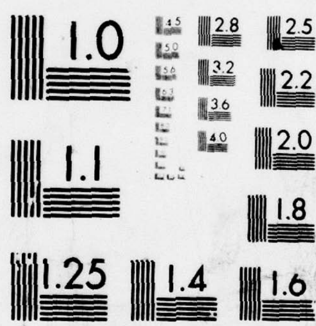

MICROCOPY RESOLUTION TEST CHART
NATIONAL BUREAU OF STANDARDS-1963-A

LEVEL IV (12)

NOSC

DDC RECEIVED NOV 1 1979 E

NOSC TD 272

AD A075945

NOSC TD 272

Technical Document 272

UNDERWATER SOUND MATHEMATICAL MODEL

Theoretical discussion

R Bell

15 August 1979

Interim Report: January 1979 — July 1979

DDC FILE COPY

Approved for public release; distribution unlimited

NAVAL OCEAN SYSTEMS CENTER
SAN DIEGO, CALIFORNIA 92152

79 11 01 015

NAVAL OCEAN SYSTEMS CENTER, SAN DIEGO, CA 92152

AN ACTIVITY OF THE NAVAL MATERIAL COMMAND

SL GUILLE, CAPT, USN
Commander

HL BLOOD
Technical Director

ADMINISTRATIVE INFORMATION

Work was done under OMN, NSEA, S, 470-TD03 by the Test Development Division, SACS/FORACS Group.

Released by
WL Burns, Head
Test Development Division

Under authority of
FD Durrett, Head
SACS/FORACS Group

UNCLASSIFIED

SECURITY CLASSIFICATION OF THIS PAGE (When Data Entered)

REPORT DOCUMENTATION PAGE

READ INSTRUCTIONS BEFORE COMPLETING FORM

1. REPORT NUMBER
NOSC Technical Document 272 (TD272)

2. GOVT ACCESSION NO.

3. RECIPIENT'S CATALOG NUMBER

4. TITLE (and Subtitle)
(6) UNDERWATER SOUND MATHEMATICAL MODEL.
Theoretical discussion.

5. TYPE OF REPORT & PERIOD COVERED
Interim - January–July 1979

6. PERFORMING ORG. REPORT NUMBER

7. AUTHOR(s)
(10) R. Bell

8. CONTRACT OR GRANT NUMBER(s)
(12) 26

9. PERFORMING ORGANIZATION NAME AND ADDRESS
Naval Ocean Systems Center
San Diego, CA 92152

10. PROGRAM ELEMENT, PROJECT, TASK AREA & WORK UNIT NUMBERS
OMN, NSEA, S, 470-TD03

11. CONTROLLING OFFICE NAME AND ADDRESS
Naval Sea Systems Command (NSEA-06H4)
Test & Support Office Washington, DC 20362

12. REPORT DATE
(11) 15 Aug [redacted]79

13. NUMBER OF PAGES
22

14. MONITORING AGENCY NAME & ADDRESS (if different from Controlling Office)

15. SECURITY CLASS. (of this report)
Unclassified

15a. DECLASSIFICATION/DOWNGRADING SCHEDULE

16. DISTRIBUTION STATEMENT (of this Report)
Approved for public release; distribution unlimited

17. DISTRIBUTION STATEMENT (of the abstract entered in Block 20, if different from Report)
(9) Interim rept. Jan-Jul 79,

18. SUPPLEMENTARY NOTES

19. KEY WORDS (Continue on reverse side if necessary and identify by block number)
Acoustic measurement
Acoustic reflection
Mathematical models
Sensor Accuracy Check Site (SACS)

(14) NOSC/TD-272

20. ABSTRACT (Continue on reverse side if necessary and identify by block number)

The physical phenomena which affect performance measurements at SACS (Sensor Accuracy Check Site) must in part be studied through the use of an acoustic mathematical model. This document derives equations for the summation of two independent acoustic waves at a point receiver, derives equations for the summation of multiple acoustic waves at a point receiver, defines a three-dimensional source cardioid, and develops general equations for the summation at a point receiver of direct and reflected path acoustic waves emanating from multiple cardioid sources.

DD FORM 1 JAN 73 1473 EDITION OF 1 NOV 65 IS OBSOLETE
S/N 0102-LF-014-6601

UNCLASSIFIED

SECURITY CLASSIFICATION OF THIS PAGE (When Data Entered)

393 159 slt

CONTENTS

Accession For
NTIS GRA&I
DDC TAB
Unannounced
Justification
By
Distribution/
Availability Codes
Dist A | Avail and/or special

INTRODUCTION

The Sensor Accuracy Check Site (SACS) is located at the Long Beach Naval Support Activity, Long Beach, California. The facility is operated by the Naval Undersea Warfare Engineering Station and technical direction is provided by Naval Ocean Systems Center, SACS/FORACS Group (Code 47). The principal purpose of SACS is to measure sonar transmitter and receiver performance for Naval combatant ships. The ship is moored with the sonar transducer positioned in the center of a 120-ft-radius pier. A 6-ft-long test transducer is mounted on a movable carriage which can traverse the perimeter of the circular pier for collection of data.

The SACS environment includes several physical phenomena which affect performance measurements. These phenomena must in part be studied with the use of an acoustic mathematical model. This document presents initial development of the model in four sections. Section I derives equations for the summation of two independent acoustic waves at a point receiver. Section II derives equations for the summation of multiple acoustic waves at a point receiver. Section III defines a three-dimensional source cardioid. Finally, section IV develops general equations for the summation at a point receiver of direct and reflected path acoustic waves emanating from multiple cardioid sources.

This is an intermediate document. A more extensive technical document will be published at a future date as the model is further developed.

SECTION I. SUMMATION OF DIRECT AND REFLECTED PRESSURE WAVES FROM A SINGLE SOURCE

TRIGONOMETRIC DERIVATION

This section provides the solution for summing two waves at a nondirectional point receiver. The first wave travels a direct path from the source. The second travels a reflected path. Both waves are projected simultaneously from a directional point source as shown in figure 1.

If the reflected path length from the source to the receiver is r_r, the direct path length from the source to the receiver is r_d, the sound pressure at the defined reference distance (eg, 1 yard) in the direction of the reflection point is A_r, and the sound pressure in the direction of the receiver is A_d, then the forms of the reflected wave and the direct wave at the point of the receiver are (see reference 1)

$$P_d = \frac{A_d}{r_d} \cos\left(\omega t - \frac{2\pi r_d}{\lambda}\right) \qquad \text{direct pressure wave} \qquad (1)$$

and $$P_r = \frac{-k\,A_r}{r_r} \cos\left(\omega t - \frac{2\pi r_r}{\lambda}\right) \qquad \text{reflected pressure wave} \qquad (2)$$

where k = reflection coefficient (minus sign indicates a 180° phase shift at the surface),
λ = wavelength,
t = travel time,
ω = angular frequency.

The directionality of the source is implied by allowing the coefficients A_d and A_r to be unequal. The two waves are traveling toward the receiver. This is observed by requiring the quantity $(\omega t - 2\pi r_d/\lambda)$ to be zero which corresponds to the peak. Then, as time t becomes larger, r_d must also become larger to keep the quantity equal to zero. Therefore, as time increases, the peak moves toward larger values of r_d; ie, toward the receiver.

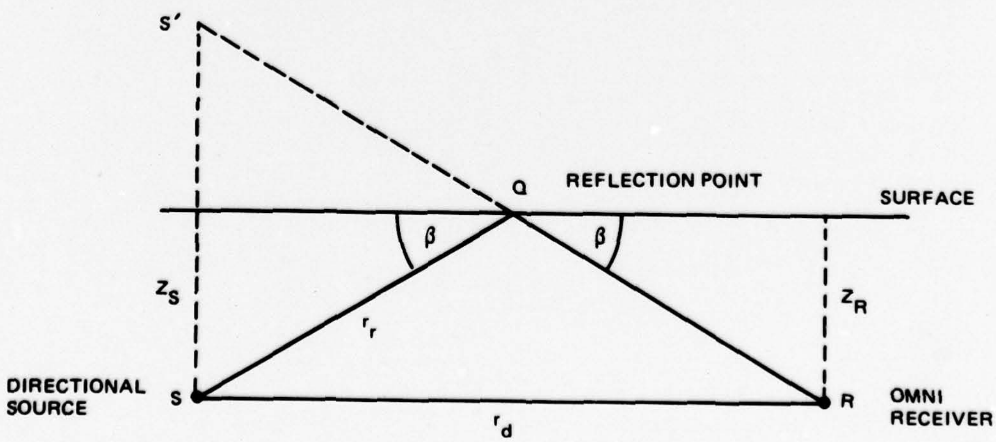

Figure 1. Interference at R between sound originating at source S and the surface image S'.

---

1. Technology of Underwater Sound, p 13, Report NADC-WR-6509, May 1965

Interference will occur at the receiver since, for example, the reflected pressure can vary from $-A_r/r_r$ to $+A_r/r_r$. The summation of the two pressure waves at the receiver can be defined as

$$P_d + P_r = \frac{A_d}{r_d} \cos\left(\omega t - \frac{2\pi r_d}{\lambda}\right) - k\frac{A_r}{r_r} \cos\left(\omega t - \frac{2\pi r_r}{\lambda}\right) \tag{3}$$

and

$$P_d + P_r = \frac{A_d}{r_d r_r} \left\{ r_r \cos\left(\omega t - \frac{2\pi r_d}{\lambda}\right) - k\frac{A_r}{A_d} r_d \cos\left(\omega t - \frac{2\pi r_r}{\lambda}\right)\right\} . \tag{4}$$

The intensity is defined as

$$I = \frac{(\text{pressure})^2}{\rho c} \tag{5}$$

where ρ = medium density and c = propagation speed. Since only the relative intensities are of interest, the factors ρ and c are not necessary and only the value for the pressure squared is needed. Therefore, squaring equation (4), we have

$$\begin{aligned}(P_d + P_r)^2 = \frac{A_d^2}{r_d^2 r_r^2} \Bigg\{ & r_r^2 \cos^2\left(\omega t - \frac{2\pi r_d}{\lambda}\right) \\ & - 2k\frac{A_r}{A_d} r_d r_r \cos\left(\omega t - \frac{2\pi r_d}{\lambda}\right) \cos\left(\omega t - \frac{2\pi r_r}{\lambda}\right) \\ & + k^2 \frac{A_r^2}{A_d^2} r_d^2 \cos^2\left(\omega t - \frac{2\pi r_r}{\lambda}\right)\Bigg\} .\end{aligned} \tag{6}$$

Using the trigonometric identity

$$\cos\alpha \cos\beta = \frac{1}{2}\cos(\alpha + \beta) + \frac{1}{2}\cos(\alpha - \beta) \tag{7}$$

or

$$\begin{aligned}\cos\left(\omega t - \frac{2\pi r_d}{\lambda}\right) \cos\left(\omega t - \frac{2\pi r_r}{\lambda}\right) = & \frac{1}{2}\cos\left(2\omega t - \frac{2\pi(r_d + r_r)}{\lambda}\right) \\ & + \frac{1}{2}\cos\left(\frac{2\pi(r_r - r_d)}{\lambda}\right) .\end{aligned} \tag{8}$$

and substituting in equation (6), we have

$$(P_d + P_r)^2 = \frac{A_d^2}{r_d^2 r_r^2} \left\{ r_r^2 \cos^2\left(\omega t - \frac{2\pi r_d}{\lambda}\right) - k\frac{A_r}{A_d} r_d r_r \cos\left(2\omega t - \frac{2\pi(r_r + r_d)}{\lambda}\right)\right.$$

$$\left. - k\frac{A_r}{A_d} r_d r_r \cos\left(\frac{2\pi(r_r - r_d)}{\lambda}\right) + k^2 \frac{A_r^2}{A_d^2} r_d^2 \cos^2\left(\omega t - \frac{2\pi r_r}{\lambda}\right)\right\} . \quad (9)$$

It is now of interest to determine the time averaged intensity at the receiver. Consider the cosine forms in equation (9) such as:

$$\cos^2(\omega t - \alpha)$$

and

$$\cos(2\omega t - \beta).$$

The time averages of these are

$$\frac{1}{\tau}\int_0^\tau \cos^2(\omega t - \alpha)\, dt \qquad \tau = \text{time of one full period} .$$

Let

$$x = \omega t - \alpha$$

$$dx = \omega dt$$

$$dt = \frac{1}{\omega} dx$$

$$\frac{1}{\omega\tau}\int_0^\tau \cos^2 x\, dx = \frac{1}{\omega\tau}\left\{\frac{1}{2}x + \frac{1}{4}\sin 2x\right\}\Big/_0^\tau$$

$$= \frac{1}{\omega\tau}\left\{\frac{1}{2}(\omega t - \alpha) + \frac{1}{4}\sin 2(\omega t - \alpha)\right\}\Big/_0^\tau$$

$$= \frac{1}{\omega\tau}\left\{\frac{1}{2}\omega\tau - \frac{\alpha}{2} + \frac{1}{4}\sin 2(\omega\tau - \alpha)\right.$$

$$\left. - 0 + \frac{\alpha}{2} - \frac{1}{4}\sin 2(0 - \alpha)\right\} . \quad (10)$$

Therefore,

$$\frac{1}{\tau}\int_0^\tau \cos^2(\omega t - \alpha)\, dt = \frac{1}{\omega\tau}\frac{1}{2}\omega\tau = \frac{1}{2} . \quad (11)$$

Next

$$\frac{1}{\tau}\int_0^{\tau} \cos(2\omega t - \beta)\, dt\,. \qquad (12)$$

Let

$$x = 2\omega t - \beta$$

$$dx = 2\omega dt$$

$$dt = \frac{1}{2\omega} dx$$

$$\frac{1}{2\omega\tau}\int_0^{\tau} \cos x\, dx = \frac{1}{2\omega\tau}\left\{\sin x\right\}\Big/_0^{\tau}$$

$$= \frac{1}{2\omega\tau}\left\{\sin(2\omega t - \beta)\right\}\Big/_0^{\tau}$$

$$= \frac{1}{2\omega\tau}\left\{\sin(2\omega\tau - \beta) - \sin(0 - \beta)\right\}. \qquad (13)$$

Therefore,

$$\frac{1}{\tau}\int_0^{\tau} \cos(2\omega t - \beta)\, dt = \text{zero}\,. \qquad (14)$$

Substituting the time averages of equations (11) and (14) into equation (9), we have

$$\overline{(P_d + P_r)^2} = \frac{A_d^2}{r_d^2\, r_r^2}\left\{\frac{r_r^2}{2} - k\,\frac{A_r}{A_d}\, r_d r_r \cos\left(\frac{2\pi(r_r - r_d)}{\lambda}\right) + \frac{k^2 A_r^2 r_d^2}{2A_d^2}\right\}; \qquad (15)$$

or,

$$\overline{(P_d + P_r)^2} = \frac{A_d^2}{2r_d^2} + \frac{k^2 A_r^2}{2r_r^2} - \frac{kA_d A_r}{r_d r_r}\cos\left(\frac{2\pi(r_r - r_d)}{\lambda}\right). \qquad (16)$$

This is the relative average intensity at the receiver. It is dependent on the path length difference $(r_r - r_d)$ and has a maximum value of $\frac{1}{2}(A_d/r_d + kA_r/r_r)^2$, which occurs when r_r is 180° longer or shorter in phase because of the 180° phase change on reflection at the surface.

COMPLEX NOTATION DERIVATION

The summation of two pressure waves may also be derived with complex notation. The basic wave equations are

$$P_d = \frac{A_d}{r_d} e^{i\left(\omega t - \frac{2\pi r_d}{\lambda}\right)} \quad \text{(real part = direct path)} \tag{17}$$

and

$$P_r = \frac{-kA_r}{r_r} e^{i\left(\omega t - \frac{2\pi r_r}{\lambda}\right)} \quad \text{(real part = reflected path)} \tag{18}$$

The sum of the pressure waves is then

$$P_d + P_r = \frac{A_d}{r_d} e^{i\left(\omega t - \frac{2\pi r_d}{\lambda}\right)} - \frac{kA_r}{r_r} e^{i\left(\omega t - \frac{2\pi r_r}{\lambda}\right)} \tag{19}$$

$$P_d + P_r = \left\{ \frac{A_d}{r_d} e^{i\left(- \frac{2\pi r_d}{\lambda}\right)} - \frac{kA_r}{r_r} e^{i\left(- \frac{2\pi r_r}{\lambda}\right)} \right\} e^{i\omega t} . \tag{20}$$

The time average intensity of the sum would be given by

$$\overline{(P_d + P_r)^2} = \frac{1}{2}(P_d + P_r) \cdot (P_d + P_r)^* \text{ (see reference 2)} \tag{21}$$

The bar indicates time averaging. The asterisk denotes the complex conjugate.

A complex number of the form $Ae^{i\theta}$ can be thought of as a vector in complex space such as shown in figure 2.

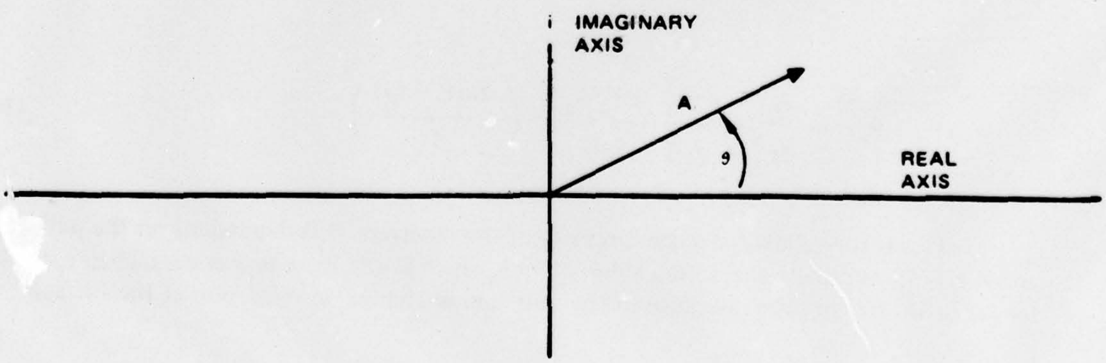

Figure 2. Plot illustrating complex numbers.

---

2. Reitz and Milford, Foundations of Electromagnetic Theory, 2nd ed, Addison-Wesley, 1967, page 337, equation (16-87)

So from Euler's formula, $Ae^{i\theta} = A\cos\theta + iA\sin\theta$ defines the two components of the vector. If two of these vectors such as P_d and P_r are to be added, then from equation (20):

$$P_d + P_r = \left\{ \frac{A_d}{r_d}\cos\left(\frac{-2\pi r_d}{\lambda}\right) + \frac{iA_d}{r_d}\sin\left(\frac{-2\pi r_d}{\lambda}\right) - \frac{kA_r}{r_r}\cos\left(\frac{-2\pi r_r}{\lambda}\right) - \frac{ikA_r}{r_r}\sin\left(\frac{-2\pi r_r}{\lambda}\right) \right\} e^{i\omega t}; \tag{22}$$

or,

$$P_d + P_r = \left\{ \left(\frac{A_d}{r_d}\cos\left(\frac{-2\pi r_d}{\lambda}\right) - \frac{kA_r}{r_r}\cos\left(\frac{-2\pi r_r}{\lambda}\right)\right) + i\left(\frac{A_d}{r_d}\sin\left(\frac{-2\pi r_d}{\lambda}\right) - \frac{kA_r}{r_r}\sin\left(\frac{-2\pi r_r}{\lambda}\right)\right) \right\} e^{i\omega t}. \tag{23}$$

The time averaged intensity would be one-half the product of equation (23) and its complex conjugate as defined in equation (21). (Note $e^{i\omega t} \cdot e^{-i\omega t} = e^0$, which becomes 1.)

Substitute

$$\cos\theta = \cos(-\theta) \tag{24}$$

and

$$-\sin\theta = \sin(-\theta) \tag{25}$$

$$\overline{(P_d + P_r)^2} = \frac{1}{2}\left\{ \left(\frac{A_d}{r_d}\cos\left(\frac{2\pi r_d}{\lambda}\right) - \frac{kA_r}{r_r}\cos\left(\frac{2\pi r_r}{\lambda}\right)\right) + i\left(\frac{kA_r}{r_r}\sin\left(\frac{2\pi r_r}{\lambda}\right) - \frac{A_d}{r_d}\sin\left(\frac{2\pi r_d}{\lambda}\right)\right) \right\} \cdot \left\{ \left(\frac{A_d}{r_d}\cos\left(\frac{2\pi r_d}{\lambda}\right) - \frac{kA_r}{r_r}\cos\left(\frac{2\pi r_r}{\lambda}\right)\right) - i\left(\frac{kA_r}{r_r}\sin\left(\frac{2\pi r_r}{\lambda}\right) - \frac{A_d}{r_d}\sin\left(\frac{2\pi r_d}{\lambda}\right)\right) \right\}. \tag{26}$$

Let:

$$\alpha = \left(\frac{A_d}{r_d}\cos\left(\frac{2\pi r_d}{\lambda}\right) - \frac{kA_r}{r_r}\cos\left(\frac{2\pi r_r}{\lambda}\right)\right) \tag{27}$$

and

$$\beta = \left(\frac{kA_r}{r_r}\sin\left(\frac{2\pi r_r}{\lambda}\right) - \frac{A_d}{r_d}\sin\left(\frac{2\pi r_d}{\lambda}\right)\right). \tag{28}$$

Then

$$\overline{(P_d + P_r)^2} = \frac{1}{2}(\alpha + i\beta) \cdot (\alpha - i\beta)$$

$$= \frac{1}{2}(\alpha^2 + \beta^2) \; . \qquad (29)$$

Substituting (27) and (28) into (29) and expanding the squared terms, we have

$$\overline{(P_d + P_r)^2} = \frac{1}{2}\left(\frac{A_d^2}{r_d^2}\cos^2\left(\frac{2\pi r_d}{\lambda}\right) - 2\frac{kA_dA_r}{r_dr_r}\cos\left(\frac{2\pi r_d}{\lambda}\right)\cos\left(\frac{2\pi r_r}{\lambda}\right)\right.$$

$$\left. + \frac{k^2A_r^2}{r_r^2}\cos^2\left(\frac{2\pi r_r}{\lambda}\right)\right) + \frac{1}{2}\left(\frac{k^2A_r^2}{r_r^2}\sin^2\left(\frac{2\pi r_r}{\lambda}\right)\right.$$

$$\left. - 2\frac{kA_dA_r}{r_dr_r}\sin\left(\frac{2\pi r_d}{\lambda}\right)\sin\left(\frac{2\pi r_r}{\lambda}\right) + \frac{A_d^2}{r_d^2}\sin^2\left(\frac{2\pi r_d}{\lambda}\right)\right) \; . \qquad (30)$$

Using $\sin^2\theta + \cos^2\theta = 1$, we have

$$\overline{(P_d + P_r)^2} = \frac{A_d^2}{2r_d^2} + \frac{k^2A_r^2}{2r_r^2} - \frac{kA_dA_r}{r_dr_r}\left(\cos\left(\frac{2\pi r_d}{\lambda}\right)\cos\left(\frac{2\pi r_r}{\lambda}\right) + \sin\left(\frac{2\pi r_d}{\lambda}\right)\sin\left(\frac{2\pi r_r}{\lambda}\right)\right) \; . \qquad (31)$$

Now, by using the trigonometric relation

$$\cos x \cos y + \sin x \sin y = \cos(x - y),$$

we obtain the following:

$$\overline{(P_d + P_r)^2} = \frac{A_d^2}{2r_d^2} + \frac{k^2A_r^2}{2r_r^2} - \frac{kA_dA_r}{r_dr_r}\cos\left(\frac{2\pi(r_r - r_d)}{\lambda}\right) . \qquad (32)$$

This is the same as the value for the relative average intensity in equation (16) found by using trigonometric expressions. The complex notation solution redefined P_d and P_r as vectors illustrated in figure 3. Referring to equations (17) and (18), the vectors have magnitudes of A_d/r_d and $-kA_r/r_r$. The angles ϕ and ψ are the angles $(\omega T - 2\pi r_d/\lambda)$ and $(\omega T - 2\pi r_r/\lambda)$. The two vectors are then added as shown in figure 4. The terms in brackets in equation (23) are the sums of C and D on the real axis and the sums of E and F on the imaginary axis. $(P_d + P_r)^2$ in equation (29) is side G^2 plus side H^2 which is $(P_d + P_r)^2$ in figure 4; the time averaging is accomplished with the 1/2.

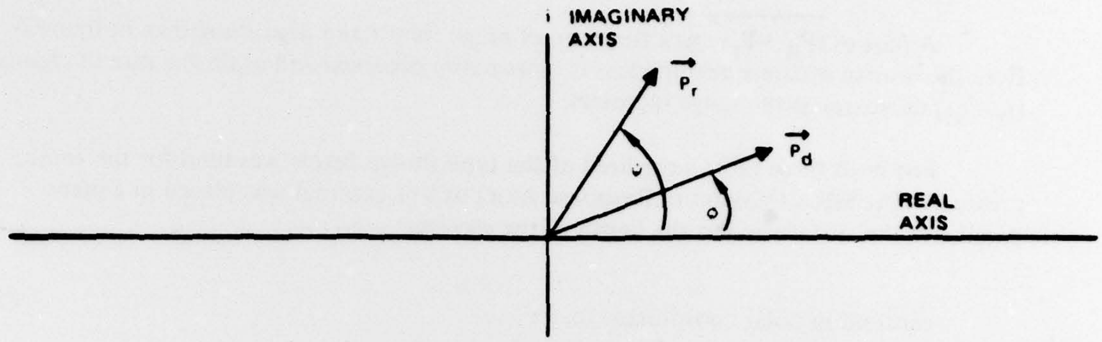

Figure 3. Geometric representation of complex numbers.

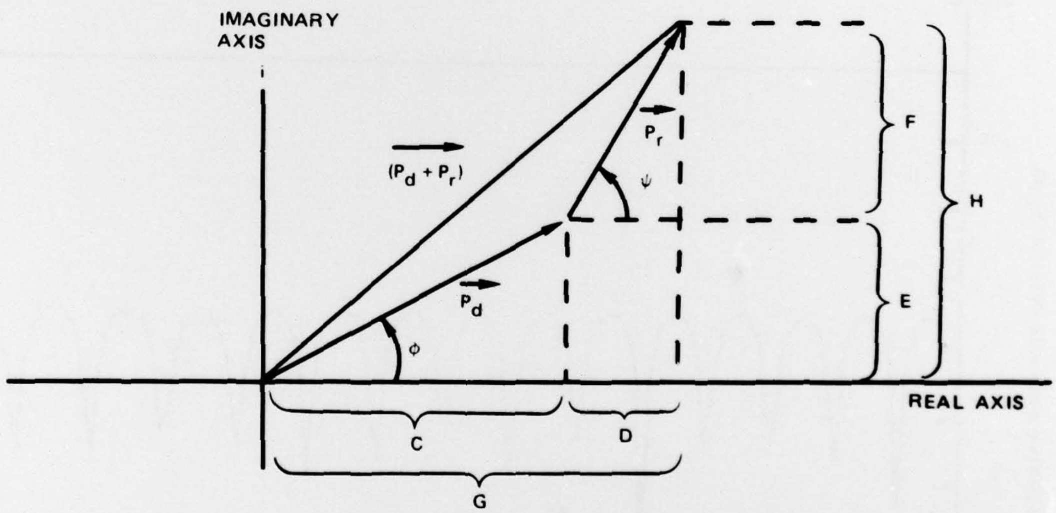

Figure 4. Graphical addition of complex numbers.

Therefore, the time averaged intensity summation of a direct and a reflected path from one source is expressed as

$$\overline{(P_d + P_r)^2} = \frac{A_d^2}{2r_d^2} + \frac{k^2 A_r^2}{2r_r^2} - \frac{kA_d A_r}{r_d r_r} \cos\left(\frac{2\pi(r_r - r_d)}{\lambda}\right) \tag{33}$$

where A_d and A_r will be determined by the cardioid of the source pressure and r_d, r_r will be determined by the geometry of the problem.

An example of the relative intensity for a source and a receiver moved in depth from the surface to 50 ft is shown in figure 5. The peaks correspond to a condition at which the quantity $(r_r - r_d)$ is equal to a multiple of one wavelength (1 ft). The peaks are broader at lower depths because the rate of change of $(r_r - r_d)$ decreases as the depth becomes larger.

A plot of $\overline{(P_d + P_r)^2}$ as a function of range for a fixed depth is shown in figure 6. Here the inverse square spreading loss is more easily observed and again the rate of change of $(r_r - r_d)$ decreases as the range increases.

For both these plots a cardioid of the type shown below was used for the source pressure. The MRA (Maximum Response Axis) of this cardioid was placed in a plane parallel to the surface and at the depth of the receiver.

cardioid in polar coordinates (ρ, θ) (34)

$$\rho = \tfrac{1}{2}(1 + \cos\theta) .$$

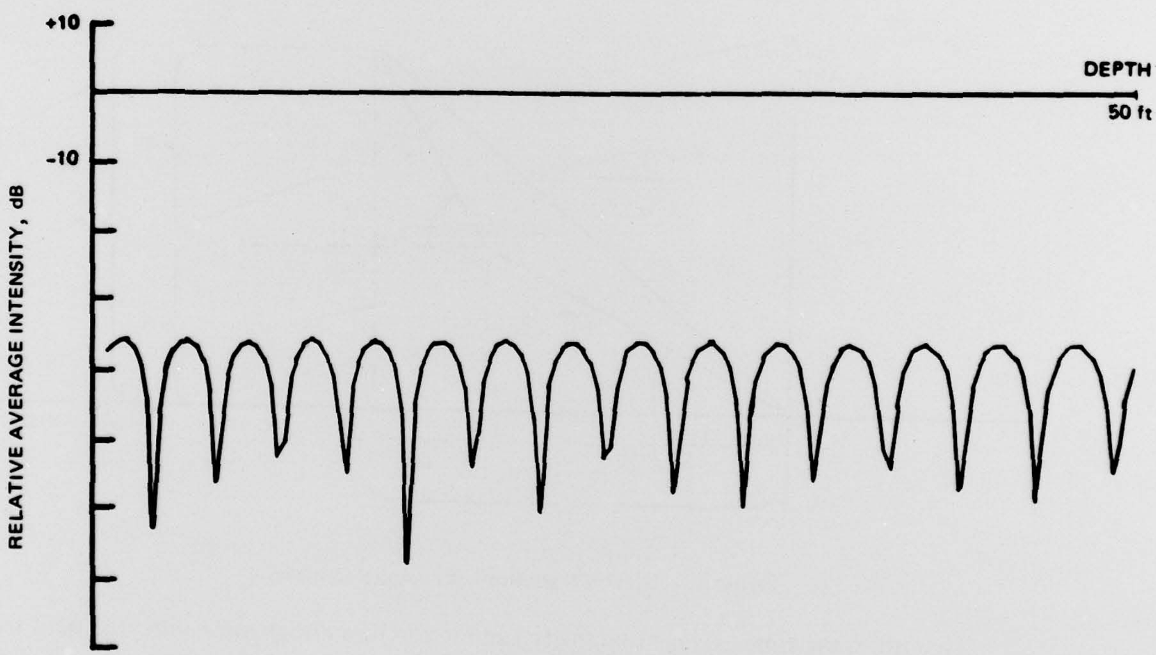

Figure 5. Relative average intensity vs depth for a single source and a point receiver at a fixed distance.

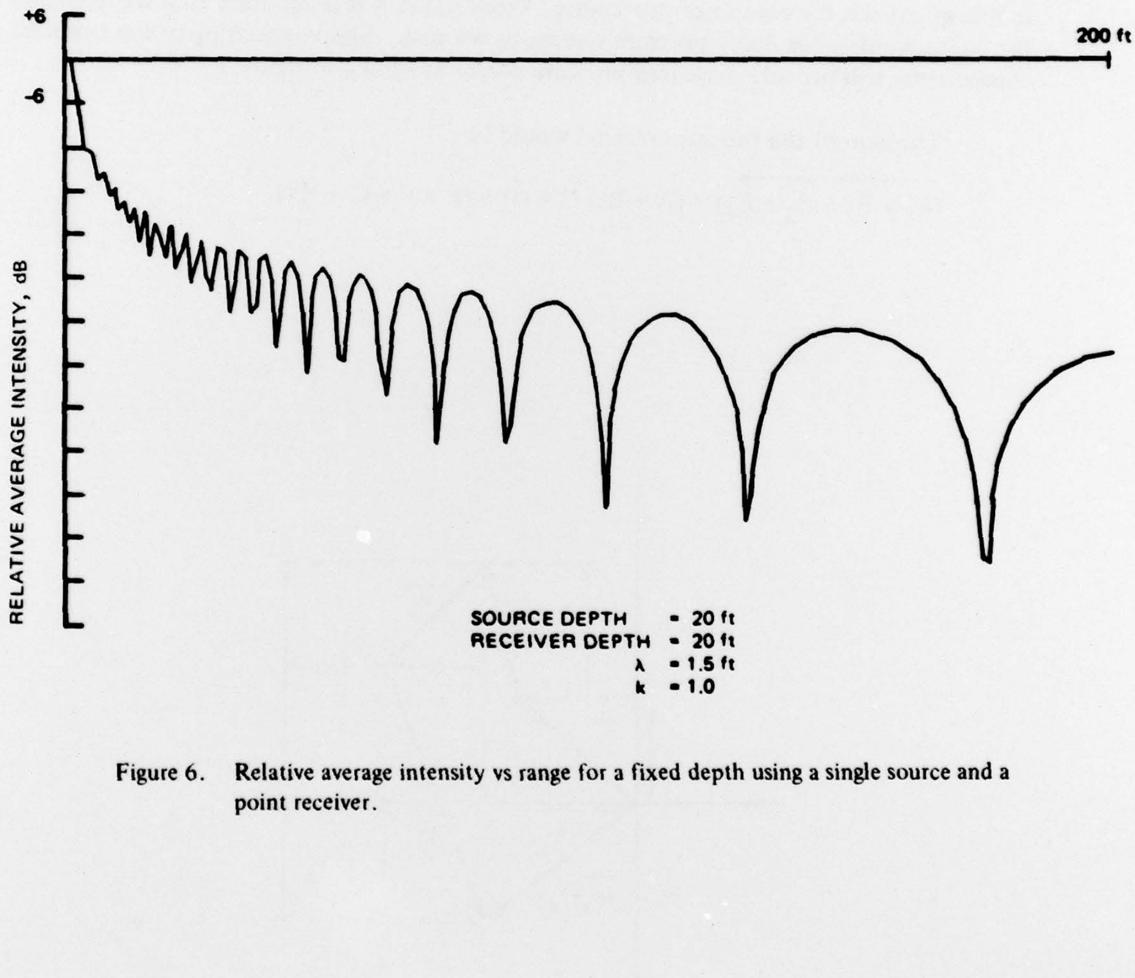

Figure 6. Relative average intensity vs range for a fixed depth using a single source and a point receiver.

SECTION II. SUMMATION OF PRESSURE WAVES FROM MULTIPLE SOURCES

Some of the theory for the single source problem is not directly applicable or is not practical for the solution of a multiple source problem, particularly if the solution is to be obtained on a computer for a large number of sources.

In equation (6) the sum of two pressure waves was squared and by the use of trigonometric identities was reduced to something which could be time averaged. If the problem required two sources, then it would be necessary to square the sum of four pressure waves, to attempt to use trigonometric identities for reduction, and, finally, to time average. This process is impossible when considering 1000 or more sources in a real sonar system.

In contrast to the trigonometric solution, complex notation provides direct and usable quantities for computer processing. From figure 4 it is apparent that we may sum the components of as many pressure vectors as we wish. Simple squaring of the summed components will provide a squared pressure vector as shown in figure 7.

The sum of the pressure vectors would be

$$\overrightarrow{(P_1 + P_2 + P_3 + P_4)} = (A + B + C + D) + (E + F + G + H)\,i\,. \tag{35}$$

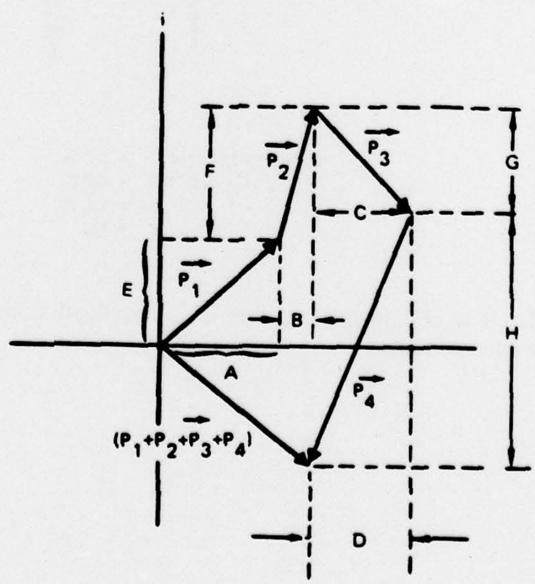

Figure 7. Plot illustrating the addition of vectors representing complex numbers.

To find the resultant pressure squared, simply square each component and add.

$$(P_1 + P_2 + P_3 + P_4)^2 = (A + B + C + D)^2 + (E + F + G + H)^2. \qquad (36)$$

The angles of the components A, B, C, etc, are defined by the quantity within the brackets in the pressure wave equations (17–20) $(\omega T - 2\pi r/\lambda)$. However, the time part was factored out in equation (20) so the angles become $(-2\pi r/\lambda)$.* The time averaged relative intensity of a number of sources with direct and reflected paths can generally be written as (reference equations (26) through (29)):

$$I = \tfrac{1}{2}\left\{\frac{A_d}{r_{Ad}}\cos\left(\frac{2\pi r_{Ad}}{\lambda}\right) - \frac{kA_r}{r_{Ar}}\cos\left(\frac{2\pi r_{Ar}}{\lambda}\right) + \frac{B_d}{r_{Bd}}\cos\left(\frac{2\pi r_{Bd}}{\lambda}\right) - \frac{kB_r}{r_{Br}}\cos\left(\frac{2\pi r_{Br}}{\lambda}\right)\ldots\ldots\right\}^2 + \tfrac{1}{2}\left\{\frac{A_d}{r_{Ad}}\sin\left(\frac{2\pi r_{Ad}}{\lambda}\right) - \frac{kA_r}{r_{Ar}}\sin\left(\frac{2\pi r_{Ar}}{\lambda}\right) + \frac{B_d}{r_{Bd}}\sin\left(\frac{2\pi r_{Bd}}{\lambda}\right) - \frac{kB_r}{r_{Br}}\sin\left(\frac{2\pi r_{Br}}{\lambda}\right)\ldots\right\}^2. \qquad (37)$$

A_d, A_r, B_d, B_r . . . will be determined by the cardioid of the source and the direction to the receiver or reflection point, and r_{Ad}, r_{Ar}, r_{Bd}, r_{Br} . . . are the path lengths and will be determined by the geometry of the problem. Also, the minus signs in the phase were left out because $\cos(-\theta) = \cos\theta$ and $\sin(-\theta) = -\sin\theta$. The quantity is squared so the sign has no effect.

SECTION III. SOURCE CARDIOID

A source may be defined by a cardioid in polar coordinates (A, ψ) as shown in figure 8. The cardioid is symmetrical about the boresight axis. The pressure A at a given point on the cardioid is a function of the angle ψ from the boresight axis and the reference pressure A_I on the axis. Thus,

$$A = A_I\left(\frac{1 + \cos\psi}{2}\right). \qquad (38)$$

At this time, the author is unsure of the effects upon the model of a choice of one source cardioid over another. Evidence by D Smith at ARL/UT and others shows that the baffle of the transducer can be included into the model by a correct choice of source cardioids. Theory for deriving a proper cardioid is treated in references 3–5. Reference 5 uses an equation similar to

$$A_I = \frac{\sin(k\ell\sin\psi)}{k\ell\sin\psi}. \qquad (39)$$

---

*Plus an additional "Initial" phase for beam forming if required.

3. Summary Tech Report of Div 6, NDRC, vol 16, Scanning Sonar Systems, 1946, chap 9
4. Directionality Patterns for Acoustic Radiation from a Source on a Rigid Cylinder, The Journal of the Acoustical Society of America, vol 24, number 1, January 1952, Laird and Cohen
5. Technical Memorandum: Some Redundancy Effects on AN/SQS-26 Performance, Tracor Document #63-233-C, 9 September 1963

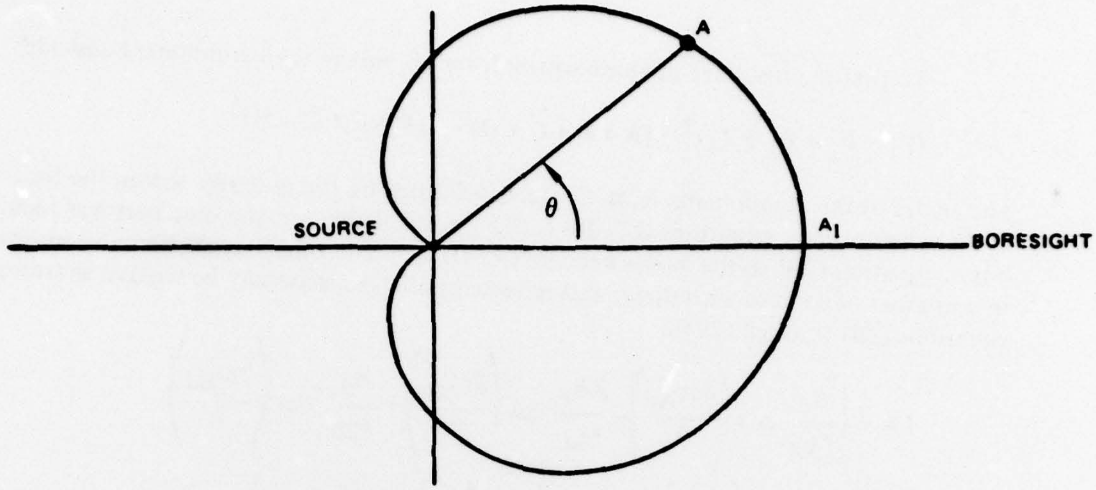

Figure 8. Cardioid in polar coordinates.

where

k = wave number $(\frac{2\pi}{\lambda})$

ℓ = element half width .

Our model is currently (19 Jan 79) using

$$\boxed{A = \frac{\sin(k\ell \sin\psi)}{k\ell\sin\psi}\left(\frac{1+\cos\psi}{2}\right)^2} \quad . \text{ (ref 3 and D Smith ARL/UT)} \tag{40}$$

Equation (40) apparently more closely represents the form of a beam generated from a two-dimensional element mounted on a solid surface than does equation (38). In the case of a circular element of 10-cm diameter, ℓ would be 5 cm. In the case of a rectangular element, ℓ would be approximately half of the diagonal dimension. Squaring the $(1 + \cos\psi)/2$ term has the effect of narrowing the cardioid. Figures 9 through 13 show examples of cardioids with ℓ/λ ratios varying from 0.25 to 5 based upon equation (40).

SECTION IV. THREE-DIMENSIONAL DETERMINATION OF PATH LENGTH AND SOURCE INTENSITY

GENERAL

A Cartesian coordinate system will be used to define the location of source and receiver elements. Horizontal and vertical angles are defined in figure 14.

Sonar systems normally employ clockwise notation, however. Therefore, input and output of data will be in the clockwise notation and converted to counterclockwise notation for the internal computational work in the computer.

The point source cardioid of figure 8 together with a point receiver of omnidirectionality will be placed in the Cartesian coordinate system as shown in figure 15.

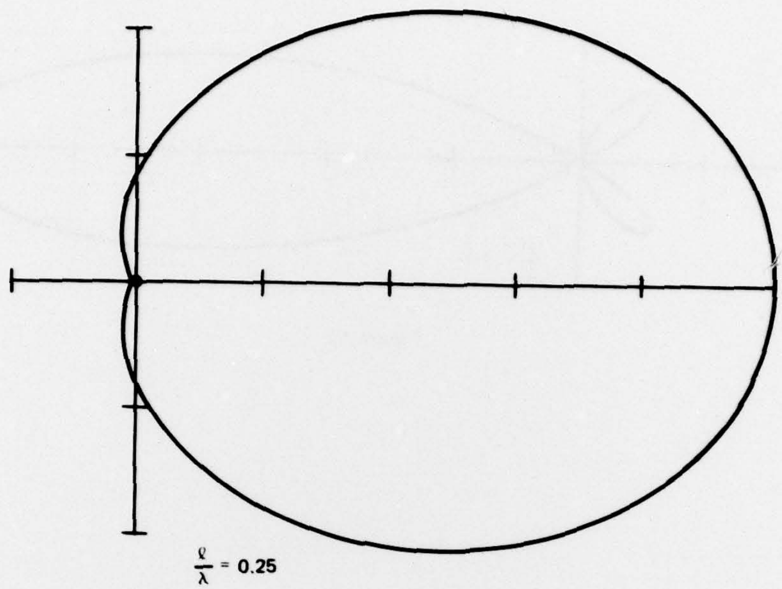

Figure 9.

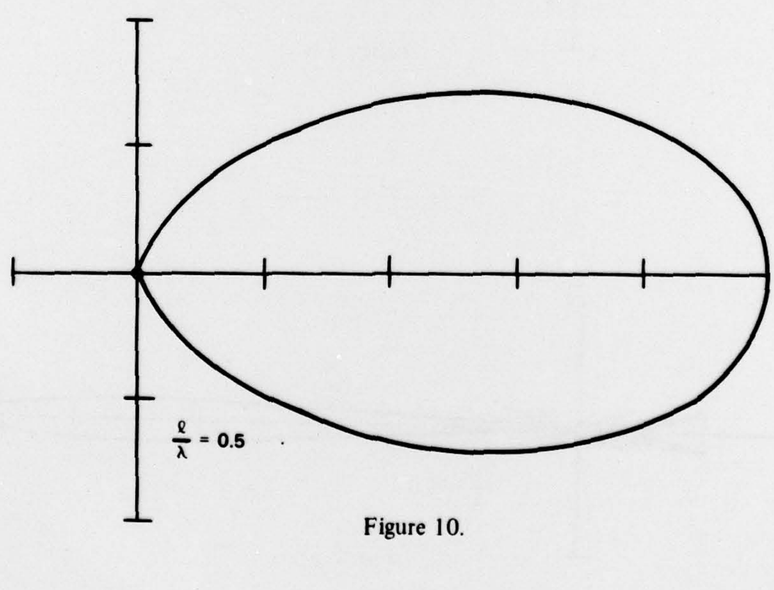

Figure 10.

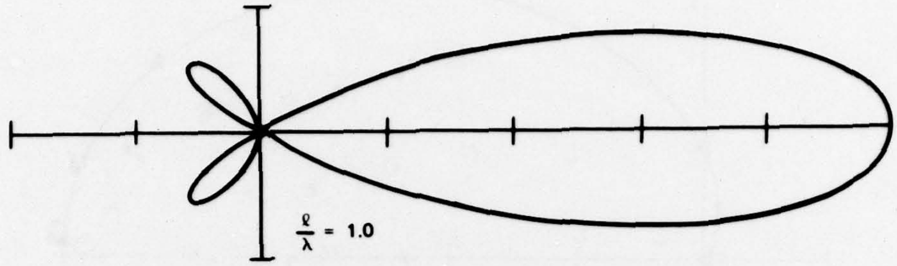

Figure 11.

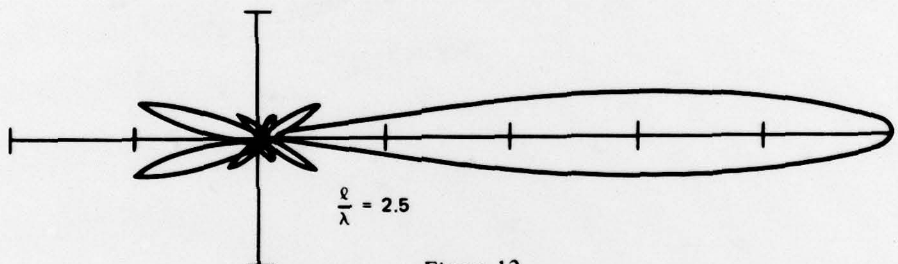

Figure 12.

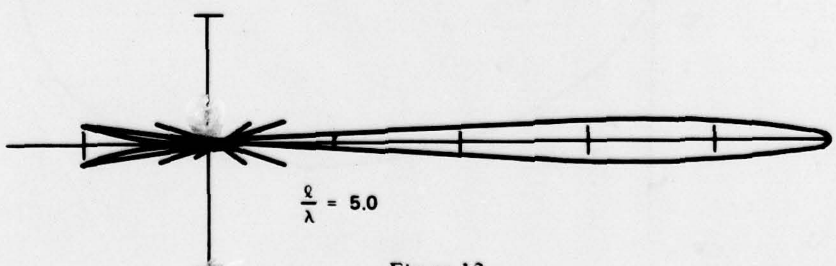

Figure 13.

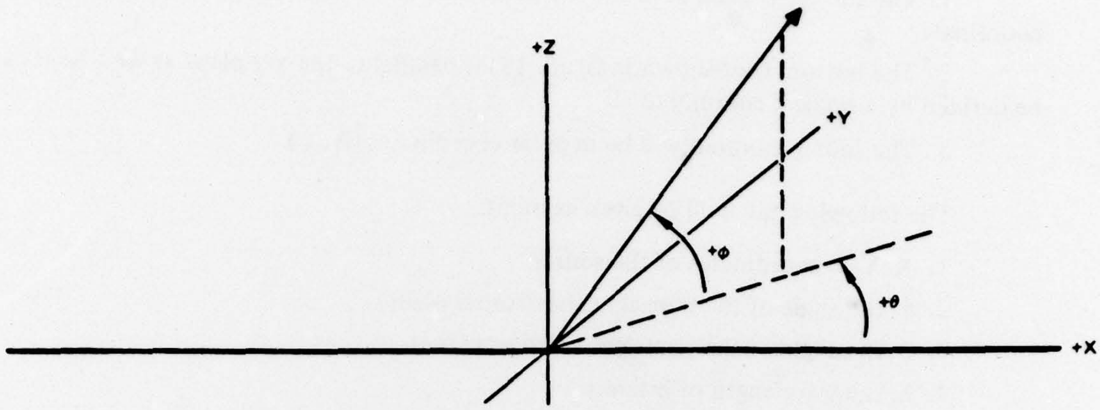

Figure 14. Three-dimensional right-hand rectangular coordinate system used; definition of horizontal and vertical angles.

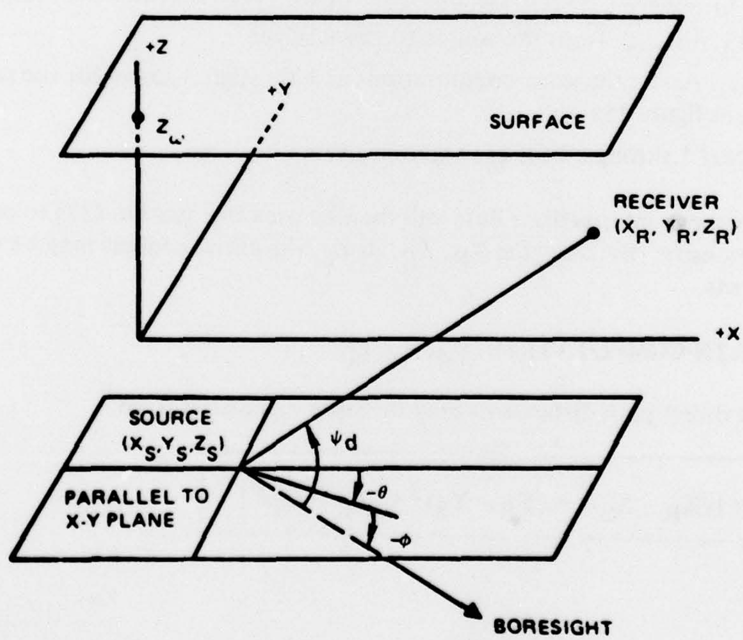

Figure 15. Configuration of source and receiver in general case.

The following assumptions apply:

1. The surface is parallel to the x-y plane and can therefore be defined by a single z coordinate.

2. The bottom (not shown in figure 15) is parallel to the x-y plane as well, so it can be defined by a single z coordinate.

3. The source cardioid will be in polar coordinates (A, ψ).

The following data will be given as input:

1. X, Y, Z coordinates of the source
2. θ, the angle of the boresight (horizontal plane)
3. ϕ, the angle of the boresight (vertical plane)
4. λ, the wavelength of interest
5. ℓ, the element half width
6. X_R, Y_R, Z_R coordinates of the receiver
7. Z_ω, coordinate of the surface

The following intermediate information must be computed:

1. ψ_d, angle from the boresight to the direct path between source and receiver
2. A_d, pressure level in the direction of the receiver (equation (40))
3. r_d, distance from the source to the receiver
4. ψ_r, A_r, r_r, the same computations as 1 through 3 above for the reflected path (not shown in figure 15)

Repeat 1 through 4 for each source given.

The above intermediate data will then be used in equation (37) to compute the resultant intensity. By changing X_R, Z_R, or Z_ω the entire process may be repeated to create beam patterns.

DIRECT PATH COMPUTATION (ψ_d, A_d, r_d)

The direct path distance r_d may be easily calculated from:

$$\boxed{r_d = [(X_R - X_S)^2 + (Y_R - Y_S)^2 + (Z_R - Z_S)^2]^{1/2}} \quad (41)$$

If the boresight is defined as vector A and the path from source to receiver is defined as vector B, then from vector theory

$$A \cdot B = |A|\,|B| \cos \psi_d. \tag{42}$$

Therefore, ψ_d may be obtained by writing the vectors for A and B. By definition

$$A = a_1 x + a_2 y + a_3 z. \tag{43}$$

If we let

$$a_1 = 1\,, \tag{44}$$

then, from figure 15 ,

$$a_2 = 1 \cdot \tan\theta \tag{45}$$

and

$$a_3 = 1 \cdot \frac{\tan\phi}{\cos\theta}\ ; \tag{46}$$

or,

$$A = x + \tan\theta y + \frac{\tan\phi}{\cos\theta} z. \tag{47}$$

Also, by definition,

$$|A| = \sqrt{a_1^2 + a_2^2 + a_3^2} \tag{48}$$

or

$$|A| = \sqrt{1 + \tan^2\theta + \left(\frac{\tan\phi}{\cos\theta}\right)^2}\ , \tag{49}$$

which may be reduced to

$$|A| = \frac{1}{\cos\theta \cos\phi}\ . \tag{50}$$

To continue:

$$B = b_1 x + b_2 y + b_3 z. \tag{51}$$

Therefore,

$$B = (X_R - X_S)x + (Y_R - Y_S)y + (Z_R - Z_S)z \tag{52}$$

and

$$|B| = \sqrt{(X_R - X_S)^2 + (Y_R - Y_S)^2 + (Z_R - Z_S)^2}\ . \tag{53}$$

Since

$$A \cdot B = a_1 b_1 + a_2 b_2 + a_3 b_3\ , \tag{54}$$

then, from equation (42),

$$\cos \psi_d = \frac{A \cdot B}{|A|\,|B|} \tag{55}$$

or

$$\boxed{\cos \psi_d = \frac{(X_R - X_S)\cos\theta\cos\phi + (Y_R - Y_S)\sin\theta\cos\phi + (Z_R - Z_S)\sin\phi}{\sqrt{(X_R - X_S)^2 + (Y_R - Y_S)^2 + (Z_R - Z_S)^2}}} \tag{56}$$

Finally, from equation (40),

$$\boxed{A_d = \frac{\sin(k\ell \sin\psi_d)}{k\ell \sin\psi_d}\left(\frac{1 + \cos\psi_d}{2}\right)^2 .} \tag{57}$$

REFLECTED PATH COMPUTATION (ψ_r, A_r, r_r)

The reflected path solution may be obtained by referring to figure 16.

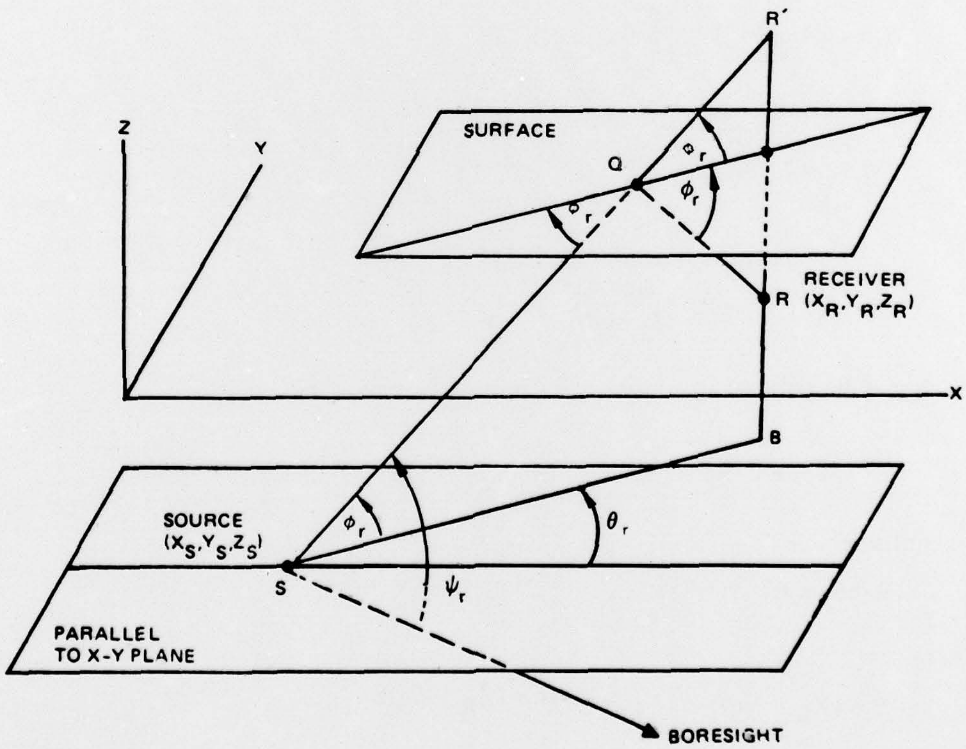

Figure 16. Reflected path from source to receiver.

The reflected path is SQR. The surface is at Z_ω. ϕ_r are all equal for obvious geometric reasons. The reflected path distance is then equal to SR′, or

$$r_r = (SB^2 + R'B^2)^{1/2} \tag{58}$$

$$SB^2 = (X_R - X_S)^2 + (Y_R - Y_S)^2 \tag{59}$$

$$R'B^2 = [Z_R - Z_S) + 2(Z_\omega - Z_R)]^2; \tag{60}$$

or,

$$\boxed{r_r = \left[(X_R - X_S)^2 + (Y_R - Y_S)^2 + (2Z_\omega - Z_R - Z_S)^2\right]^{1/2}.} \tag{61}$$

ψ_r is defined as the angle between the boresight and the reflected path in the direction of SQ of figure 16. As in the previous section, two vectors must be defined. Vector A is the boresight vector and is identical to that of equations (47) and (50) referenced to figure 15. Repeated:

$$A = x + \tan\theta y + \frac{\tan\phi}{\cos\theta} z \tag{62}$$

$$|A| = \frac{1}{\cos\theta \cos\phi} \quad . \tag{63}$$

Vector B may be similarly expressed in terms of ϕ_r and θ_r as shown in figure 16.

$$B = x + \tan\theta_r y + \frac{\tan\phi_r}{\cos\theta_r} z \quad . \tag{64}$$

From figure 16,

$$\tan\theta_r = \frac{(Y_R - Y_S)}{(X_R - X_S)} \quad , \tag{65}$$

$$\cos\theta_r = \frac{X_R - X_S}{\left[(X_R - X_S)^2 + (Y_R - Y_S)^2\right]^{1/2}} \quad , \tag{66}$$

and

$$\tan\phi_r = \frac{(2Z_\omega - Z_S - Z_R)}{\left[(X_R - X_S)^2 + (Y_R - Y_S)^2\right]^{1/2}} \quad . \tag{67}$$

Substituting into equation (64), we have

$$B = x + \frac{(Y_R - Y_S)}{(X_R - X_S)} y + \frac{(2Z_\omega - Z_S - Z_R)}{(X_R - X_S)} z \tag{68}$$

and

$$|B| = \sqrt{1 + \left(\frac{Y_R - Y_S}{X_R - X_S}\right)^2 + \left(\frac{2Z_\omega - Z_S - Z_R}{X_R - X_S}\right)^2} \; . \tag{69}$$

Finally, substituting equations (62), (63), (68), and (69) into equations (54) and (55) and simplifying, we have

$$\boxed{\cos \psi_r = \frac{(X_R - X_S) \cos \theta \cos \phi + \phi (Y_R - Y_S) \sin \theta \cos \phi + (2Z_\omega - Z_S - Z_R) \sin \phi}{\sqrt{(X_R - X_S)^2 + (Y_R - Y_S)^2 + (2Z_\omega - Z_S - Z_R)^2}}} \tag{70}$$

and, of course,

$$\boxed{A_r = \frac{\sin (k\ell \sin \psi_r)}{k\ell \sin \psi_r} \left(\frac{1 + \cos \psi_r}{2}\right)^2 .} \tag{71}$$